



## HORIZONTAL CONCRETE SLABS AS PASSIVE SOLAR COLLECTORS

E. BILGEN<sup>†</sup> and M.-A. RICHARD

Ecole Polytechnique, Box 6079, centre-ville, Montreal, Quebec H3C 3A7, Canada

Received 23 May 2001; revised version accepted 16 December 2001

Communicated by ANDREAS ATHIENITIS

**Abstract**—Natural convection, radiation and conduction heat transfer on horizontal concrete slab systems is experimentally studied. The system was a 0.78 m long, 0.40 m wide and 0.10 m thick concrete slab. A heat source was used to impose a constant heat flux which could be varied from about 200 to 700 W/m<sup>2</sup>. Temperatures at various points and heat flux by natural convection at the horizontal surface were measured. Using various assumptions, the system was also analyzed theoretically. It is found that the mathematical model to study the transient heat transfer in the slab system was satisfactory to predict its thermal behavior in various conditions. An empirical correlation for natural convection on the horizontal concrete slab was derived and used in the analysis. The results showed that the incident energy on the concrete slab was not a parameter affecting strongly the absorbed heat by the slab, the radiation heat losses made about 60% while those by natural convection 40%, and the major energy storage–restitution was taking place during the first 3 to 4 h. The optimization of energy storage density and the thermal performance was also discussed and various parameters affecting them were defined. © 2002 Elsevier Science Ltd. All rights reserved.

### 1. INTRODUCTION

It is well known that massive walls are used in passive solar heating and ventilating systems (Bilgen and Michel, 1979). In most of the applications of this type the concrete collectors are usually in vertical or near vertical position.

Concrete solar collectors used in horizontal or near horizontal position, which may be classified as active systems, are proposed for various other applications: for swimming pool heating using pavements (Sedgwick and Patrick, 1981), various domestic applications (Turner, 1986, 1987), domestic water heating (Nayak *et al.*, 1989; Bopshetty and Nayak, 1992; Chaurasia, 2000), to replace conventional solar collectors for heating applications and for water heating (Al-Saad and Jubran, 1994; Jubran and Al-Saad, 1994), and use as building components (Sokolov and Reshef, 1992).

A first application of active concrete solar collectors in the literature seems to be that of Olive (1977) who investigated their steady state behavior. Later, Sedgwick and Patrick (1981) studied experimentally swimming pool heating by

use of a grid of plastic pipes laid under an asphalt surface. They compared their results with those theoretically obtained using a simple model and found that the system was technically feasible and cost effective compared to a conventional swimming pool solar heater. Turner (1986, 1987) studied concrete collectors for applications varying from de-icing of roads and bridges to water heating for various use. He has also done some simple analysis and found that these systems may be suitable for the applications he was aiming towards.

Later studies have aimed to manufacture solar collectors using local materials and to provide domestic hot water with acceptable efficiencies. Nayak *et al.* (1989) carried out experimental studies using PVC tubes embedded in wire mesh reinforced concrete. They considered tube-to-tube spacing as a parameter and established optimal pitch and also studied pressure drop through the tube network. In a later study, Bopshetty and Nayak (1992) carried out a transient analysis of concrete solar collectors with pipe embedded, involving two-dimensional conduction. They validated their theoretical results with experimental data. They also did a sensitivity analysis to study the effect of various governing parameters on the collector performance. Chaurasia (2000), on the other hand, did a similar experimental study with aluminum tubes embedded over the surface of concrete collectors. With the same aim, Al-Saad

<sup>†</sup> Author to whom correspondence should be addressed.  
Shizuoka University, Faculty of Engineering, 5-3-1  
Johoku, Hamamatsu, Japan. Tel./fax: +81-53-478-1605;  
e-mail: tebilge@ipc.shizuoka.ac.jp

and Jubran (1994) and Jubran and Al-Saad (1994) studied experimentally and theoretically concrete solar collectors with various types of tubes and showed that these collectors could be easily manufactured using local materials. They found that the thermal performance of the concrete collectors could be as high as 40% although, as expected, the time constant was also high. Sokolov and Reshef (1992) investigated thin concrete collectors with embedded tubes, did a transient analysis and concluded that these collectors could be used as building components providing a low cost energy collection means.

The literature review shows that concrete solar collectors with tubes embedded and used in quasi-horizontal position have been studied experimentally as well as theoretically. However, passive systems consisting of concrete solar collectors in horizontal or quasi-horizontal position have not been considered. De-icing, melting of snow and maintaining a temperature slightly above that of ambient on roads, bridges and airport runways may help to alleviate various problems and also may offer an ecological solution. The purpose of the present investigation is to study experimentally and theoretically a passive system consisting of a horizontal concrete slab and establish the relative influence of various parameters on the thermal performance.

## 2. EXPERIMENTAL APPARATUS

A schematic of the apparatus used in the experiments is shown in Fig. 1. The massive slab was made of concrete. Its dimension was  $W=0.40$  m wide,  $H=0.78$  m long and  $L=0.10$  m thick. Its horizontal and vertical extremities were insulated by 0.05-m polystyrene insulation substrate. The slab was rested on a 0.05-m polystyrene insulation. Thermocouples were attached at the geometrical center of the slab, at three levels, at the surface, mid-level and the bottom. The holes were drilled with a mill to ensure accurate location of the temperature measurements. The thermocouples were from fine,  $1.27 \times 10^{-3}$ -m diameter copper-constantan thermocouple wires and attached with epoxy and later covered with concrete. The ambient air temperature far from the apparatus and the temperatures of the supporting surface of the heat source and surrounding surfaces were measured using thermocouples. The convection heat flux at the surface was measured using a  $0.1 \text{ m} \times 0.1 \text{ m} \times 10^{-4}$  m thick heat flux meter, the resolution of which was  $\pm 1 \text{ W/m}^2$ . The heat flux meter was made of copper with an emissivity  $\epsilon = 0.05$ . It was installed on the surface and at the geometrical center of the slab. In a preliminary study, temperature distributions in the slab were measured at

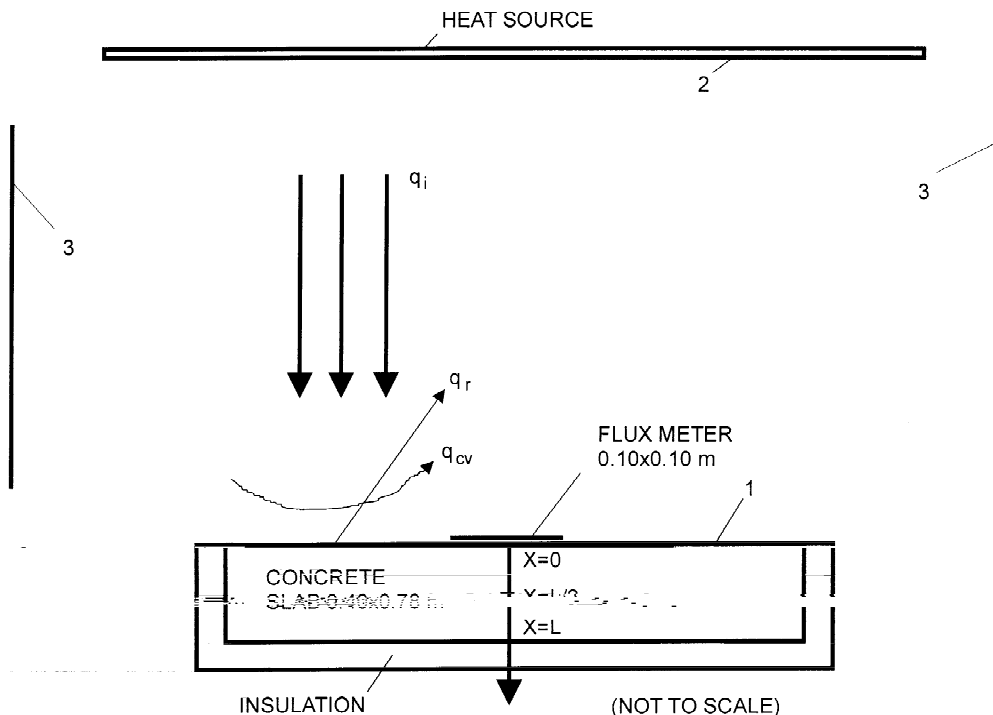


Fig. 1. Schematic of the test apparatus, the coordinate system and the parameters.

two locations one with the sensor and the other without. It was determined that the sensor on the concrete surface did not change conduction heat transfer characteristics of the concrete during the heating period.

The heat source was a multiple-lamp design system. Twenty-five 75-W halogen light bulbs were installed in a staggered form in an area of 1 m by 1 m. It is known that radiation produced by halogen light bulbs has a spectral distribution similar to solar radiation in the wavelength range of 0.20–2.7  $\mu\text{m}$ , which contain 97% of the energy in solar radiation (Kenny and Davidson, 1994). A rheostatic control was used to provide the desired heat flux for each experiment, which varied from about 200 to 700  $\text{W}/\text{m}^2$ . The rheostatic set points, which were determined using a voltmeter, were calibrated using a radiometer at the center of the receiving surface level of the apparatus, which was at 1 m distance. The heat flux measurements were made on the receiving surface placed at 1 m, and using a mesh of 0.1 m by 0.1 m for traversing. It was found that at the receiving surface level, the fluctuation of the heat flux was less than  $\pm 2.5\%$  over the average heat flux on the surface.

The slab was made of unpainted concrete. Thermo-physical property data taken from the literature were: density  $\rho = 2300 \text{ kg}/\text{m}^3$ , which was confirmed by measurements, thermal capacity  $c_p = 880 \text{ J}/\text{kg K}$ , thermal conductivity  $k = 1.4 \text{ W}/\text{m K}$ , and the emissivity  $\epsilon = 0.88$ . Although its humidity content was not measured, qualitatively it appeared to be dry due to cyclic heating prior to the present experimental study.

Using the theoretical model explained later, a sensitivity study was carried out with the thermo-physical property parameters. The results are presented in Table 1. It is seen that the influence of these parameters on the results, in particular, on the temperature of the slab is negligibly small. On the natural convection heat transfer, it is at acceptable levels varying from  $\pm 2.7$  to 3.9%. The influence of the emissivity on the radiation and as a result on the energy absorbed by the slab is  $\pm 4.5\%$  at most. Therefore, it was concluded that these property data from the literature could be used without further consideration.

The experiment was carried out in a laboratory

free of ventilation currents. The working fluid was air. The ambient air temperature varied less than 0.2 K through the experimentation, which took typically 24 h, which included a heating experiment of about 12 h and cooling of 12 h. A data logging system consisting of multiplex carts and a PC was used to collect data of transient temperatures and heat flux at the slab's surface. The experimental error in temperature measurements was estimated to be  $\pm 2.4^\circ\text{C}$ , which resulted from various sources: compensation error  $\pm 1^\circ\text{C}$ , linearization error  $\pm 0.03^\circ\text{C}$ , offset error  $\pm 0.76^\circ\text{C}$ , thermocouple error  $\pm 2^\circ\text{C}$ . The error in heat flux measurement was estimated to be  $\pm 1.6 \text{ W}/\text{m}^2$ , which is based on  $\pm 1.1 \text{ W}/\text{m}^2$  compensation error,  $\pm 0.6 \text{ W}/\text{m}^2$  read out instrument error and  $\pm 1 \text{ W}/\text{m}^2$  heat flux sensitivity.

### 3. DATA REDUCTION

The aim of the study was to obtain and examine transient temperatures at various points shown in Fig. 1 and heat flux from the surface of the slab during the cooling period, as a function of the incident heat flux and ambient temperature. Experiments were carried out starting from a state at which the initial conditions of the apparatus were known and recorded. At the desired incident heat flux on the system, the experiment was continued until a quasi-steady state condition was reached, which took about 10 to 15 h. During the heating period the transient temperatures at various points were recorded. At the end of the heating period, the heat source was turned off and the slab was left to cool, which took about 10 to 15 h. During this period the temperatures and the heat flux were recorded. They will be presented in appropriate figures, after analyzing the combined heat transfer on a horizontal concrete slab system.

### 4. ANALYSIS

It is assumed that (i) surfaces are diffuse and gray; (ii) they have uniform temperatures and radiosities; (iii) surroundings are large and isothermal.

With these assumptions, the following energy conservation equations and the heat transfer by

Table 1. Influence of various parameters on  $T(x = 0)$ ,  $T(x = L)$  and natural convection coefficient

Parameter	Value	% Variation	$T(x = 0)$ %	$T(x = L)$ %	$h$ %
$\epsilon_i$	0.88	$\pm 4.5$	$\pm 0.2$	$\pm 0.2$	$\pm 3.9$
$k$	1.4 $\text{W}/\text{m K}$	$\pm 14$	$\pm 0.19$	$\pm 0.2$	$\pm 2.7$
$\rho$	2300 $\text{kg}/\text{m}^3$	$\pm 9$	$\pm 0.27$	$\pm 0.37$	$\pm 4.5$
$c_p$	880 $\text{J}/\text{kg K}$	$\pm 4.5$	$\pm 0.14$	$\pm 0.19$	$\pm 2.3$

convection, radiation and conduction on surfaces 1 to 3 (see Fig. 1), are written.

Energy balance on surface 1 is

$$q_i = q_{cv}(t) + q_r(t) + q_c(t). \tag{1}$$

Heat transfers by natural convection, radiation and conduction are computed.

Heat transfer by natural convection is calculated using an empirical relation obtained in the actual experimental conditions. To obtain the data, the heat flux meter installed on the horizontal surface of the concrete slab discussed earlier was used. The Rayleigh number was varied from  $10^6$  to  $5 \times 10^6$  and the correlation so obtained is shown in Fig. 2

$$Nu = 0.44Ra^{1/4}. \tag{2}$$

It is noted that as expected, Eq. (2) gives about 18.5% lower values than that in the literature for laminar natural convection on horizontal plates (LLoyd and Moran, 1974). The reason for this difference is due to the fact that the local heat transfer coefficient is higher near the sides of a horizontal plate and decreases at the central region as shown recently (Pretot *et al.*, 2000). The measurements in this study were made at the center of the slab, as a result of which it is expected that the heat transfer by natural convection at the center of the slab be lower with respect

to its average value over the entire area. It is also noted that the correlation of the literature was obtained using small size horizontal plates of various geometry and the side effects discussed above were probably not present.

The heat transfer by natural convection was then calculated from

$$q_{cv}(t) = h(t)(T_1(t) - T_a(t)) \tag{3}$$

$T_a(t)$  is measured and known at a given time.

Heat transfer by radiation is calculated by considering the system in Fig. 1 as a three-surface enclosure. Radiation exchange between surfaces results in a system of four simultaneous linear equations of the form  $[a][x] = [b]$  with unknowns of  $q_{r1}(t)$ ,  $J_1(t)$ ,  $J_2(t)$  and  $J_3(t)$  in  $[x]$

$$\left. \begin{aligned} q_{r1}(t) + \frac{\epsilon_1}{1-\epsilon_1} J_1(t) &= \frac{\epsilon_1 E_{b1}(t)}{1-\epsilon_1} \\ \left( \frac{\epsilon_1}{1-\epsilon_1} + F_{12} + F_{13} \right) J_1(t) - F_{12} J_2(t) + F_{13} J_3(t) &= \frac{\epsilon_1 E_{b1}(t)}{1-\epsilon_1} \\ -F_{12} J_1(t) - \left( \frac{\epsilon_2}{1-\epsilon_2} + F_{21} + F_{23} \right) J_2(t) - F_{23} J_3(t) &= \frac{\epsilon_2 E_{b2}(t)}{1-\epsilon_2} \\ -F_{31} J_1(t) - F_{32} J_2(t) - \left( \frac{\epsilon_3}{1-\epsilon_3} + F_{31} + F_{32} \right) J_3(t) &= \frac{\epsilon_3 E_{b3}(t)}{1-\epsilon_3} \end{aligned} \right\} \tag{4}$$

where the black body powers for surfaces 1, 2 and 3 are obtained from

$$E_{b1}(t) = \sigma T_1^4(t) \tag{5}$$

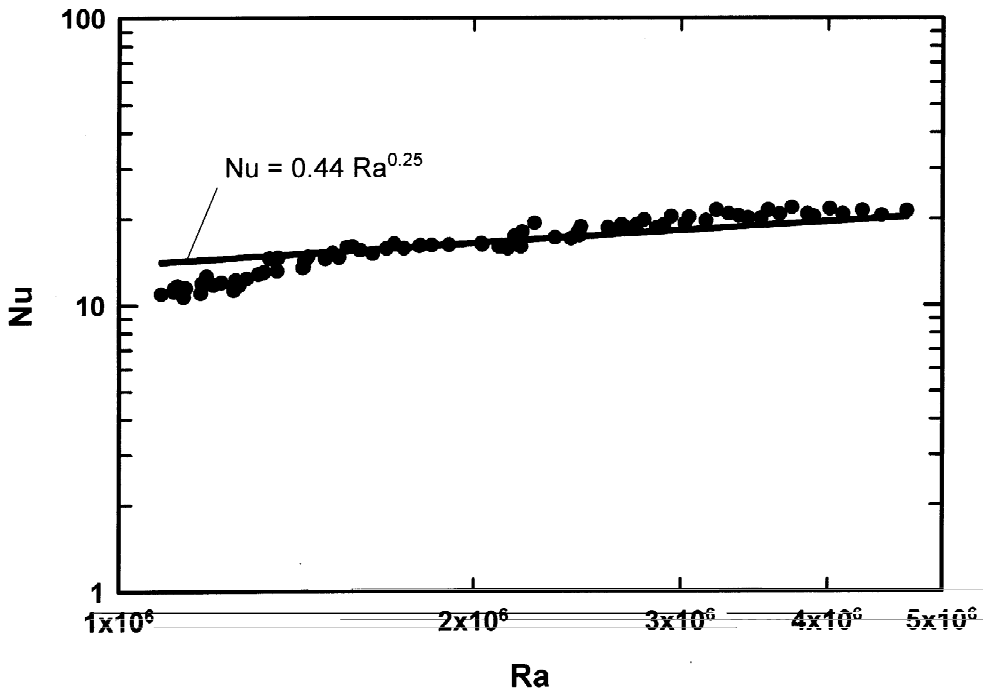


Fig. 2.  $Nu$  as a function of  $Ra$  for natural convection on the horizontal concrete slab.

$$E_{b2}(t) = \sigma T_2^4(t) \tag{6}$$

$$E_{b3}(t) = \sigma T_3^4(t). \tag{7}$$

In Eq. (4), the view factors,  $F_{ij}$ , are evaluated as  $F_{32} = F_{31} = 0.122$ ,  $F_{12} = F_{21} = 0.079$ , and  $F_{13} = F_{23} = 0.921$  (Siegel and Howell, 1981). Temperatures  $T_2(t)$  and  $T_3(t)$  are measured and known at a given time.  $T_1(t)$  is determined from the unsteady conduction equation. The radiation from surface 1,  $q_{r1}$ , is obtained from the solution of the system, Eq. (4).

$T(x, t)$  are calculated from the unsteady conduction equation. With no internal heat generation and the assumption of constant thermal conductivity, the one dimensional heat conduction equation is

$$\frac{\partial^2 T}{\partial x^2} = \frac{1}{\alpha} \frac{\partial T}{\partial t}. \tag{8}$$

The initial condition is specified as  $T(x, 0) = T_i(x)$ . Assuming that the surface at  $x = L$  is adiabatic, the boundary conditions are

$$\left. \begin{aligned} -k \frac{\partial T}{\partial x} \Big|_{x=0} &= q_i - q_{cv}(t) - q_r(t) \\ \frac{\partial T}{\partial x} \Big|_{x=L} &= 0 \end{aligned} \right\} \tag{9}$$

Eq. (8) is solved by using an explicit finite difference method and  $T(x, t)$  is obtained. It is noted that the stability criteria for this method are

$$\left. \begin{aligned} Fo &= \frac{\alpha \Delta t}{(\Delta x)^2} \leq 0.5 \quad \text{for interior nodes} \\ Fo(1 + Bi) &\leq 0.5 \quad \text{for the surface node} \end{aligned} \right\} \tag{10}$$

The numerical calculations were carried out with five nodal points in the slab and using time intervals of  $\Delta t = 120$  s. Using typical values, it is found that the order of magnitudes of  $Fo$  and  $Bi$  are both  $10^{-1}$  and these criteria are satisfied.

### 5. RESULTS AND DISCUSSION

Ten experiments were carried out using heat flux from 200 to 700 W/m<sup>2</sup> as described earlier. The results are reduced and together with the theoretical ones are presented in Figs. 2–8.

Figs. 3 and 4 show typical results with  $q_i = 381.6$  W/m<sup>2</sup> for the duration of the experiment. Experimental and theoretical temperatures at the surface, mid-level and at the bottom of the concrete slab are plotted as a function of time in Fig. 3. The deviations between theoretical and experimental data are about  $\pm 2.4$  K, which is less

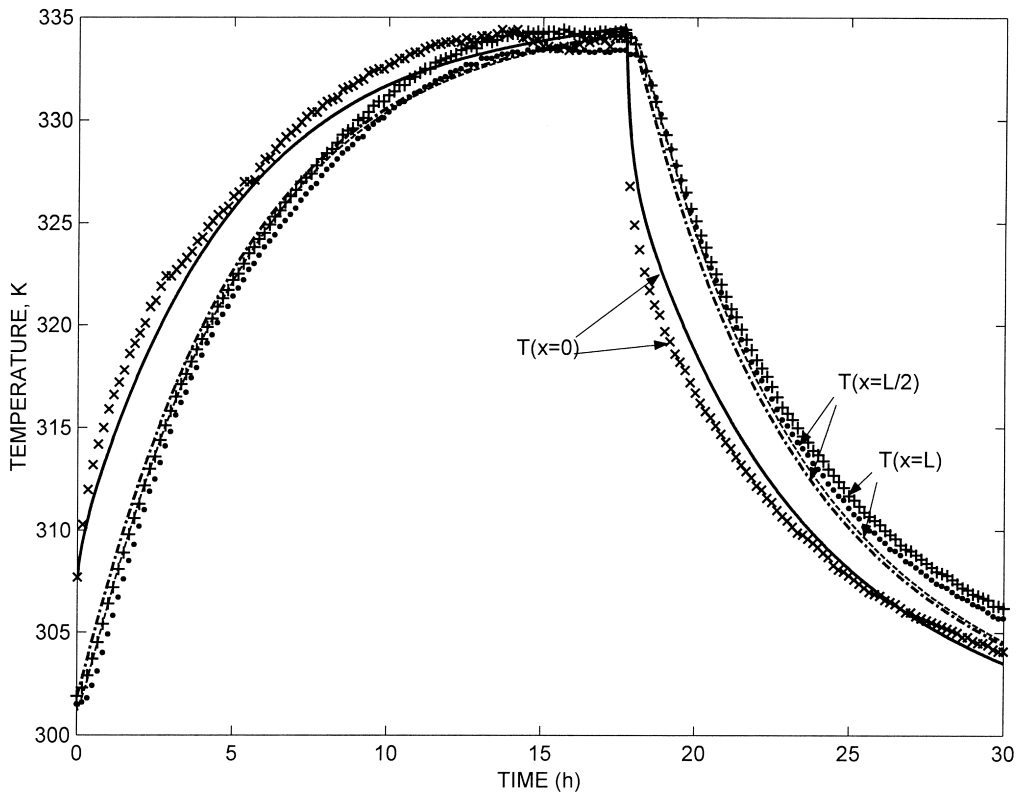


Fig. 3. Typical experimental and theoretical results for  $T(x, t)$  and  $q_i = 381.6$  W/m<sup>2</sup>.

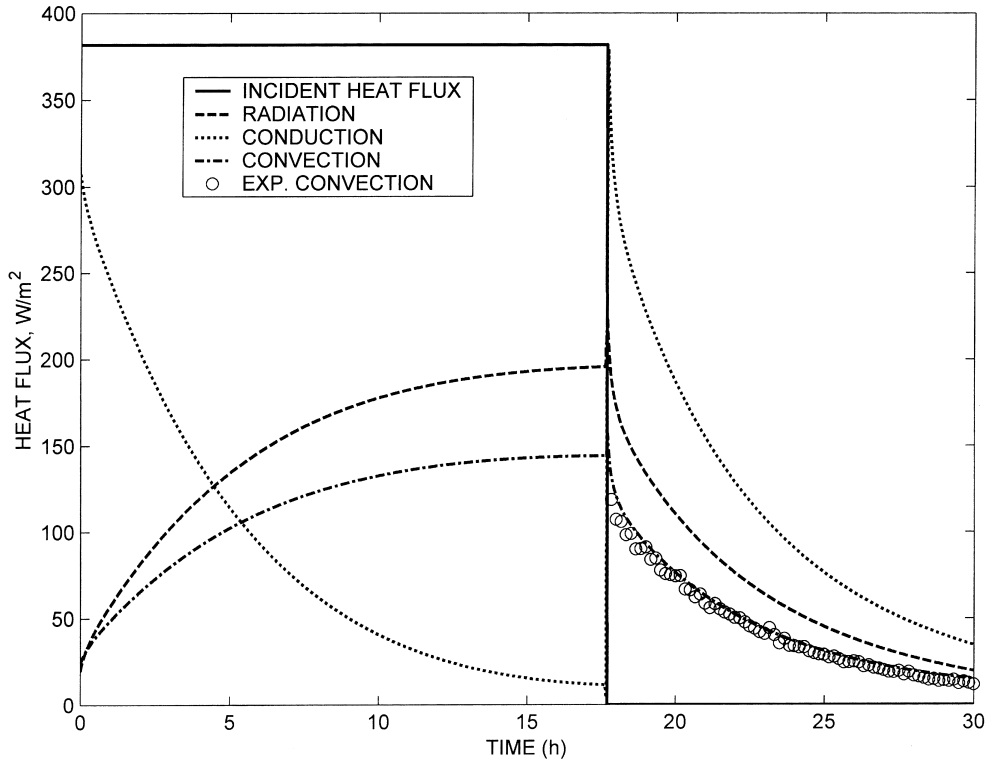


Fig. 4. Experimental and theoretical heat flux at surface 1 as a function of time with  $q_i = 381.6 \text{ W/m}^2$ .

than the experimental error predicted. All the other cases showed similar trends. It is seen that a quasi-steady state has been reached for this case within  $\pm 2 \text{ K}$  at about 12 h, and the heating period stopped at about 18 h. The cooling period has been about 13 h. The theoretical surface temperature seems to be over predicted during the first 15 h, but the final 3 h have a better agreement. Later during the cooling period, the theory underpredicts, but again with good agreement at later times. The reason may be due to uncertainties of

the non-linear boundary conditions at the surface. In fact, the theoretical results at the mid and bottom levels are in better agreement, since the influence of the uncertainties on the surface is somewhat reduced inside the slab.

Theoretical and experimental heat fluxes as a function of time are shown in Fig. 4. The incident heat flux,  $q_i$ , theoretical heat fluxes on the surface,  $q_r$ ,  $q_{cv}$  and  $q_c$  during the experimentation and the experimental heat flux by natural convection during the cooling period are presented. It is seen that 50% of the incident heat flux is absorbed

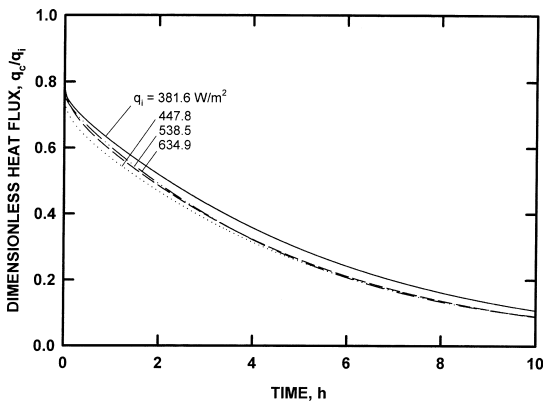


Fig. 5. Theoretical dimensionless heat flux absorbed by surface 1 for various  $q_i$  as a function of time and at the experimental conditions.

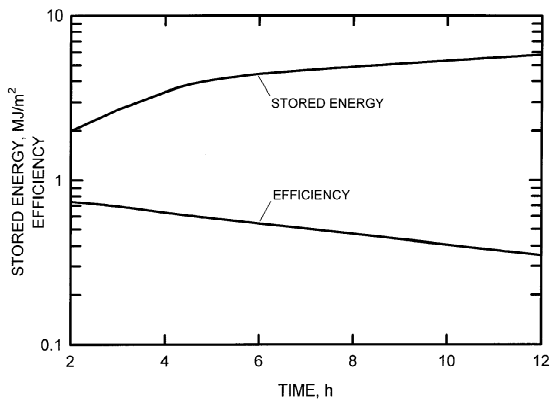


Fig. 6. Stored energy and efficiency as a function of time with  $q_i = 381.6 \text{ W/m}^2$ .

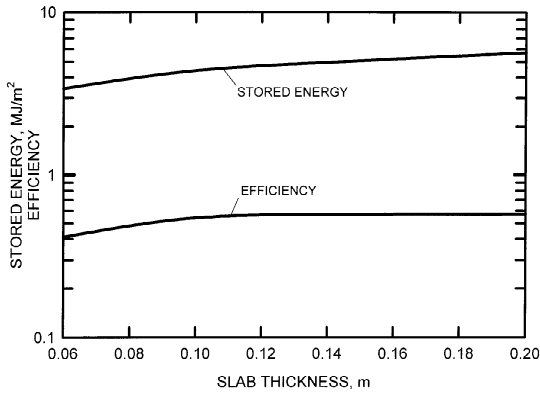


Fig. 7. Stored energy and efficiency as a function of slab thickness at  $t=6$  h with  $q_i = 381.6 \text{ W/m}^2$ .

within 3.5 h during which the losses by radiation and convection are relatively small. Thereafter, the losses continue to increase as a result of which the absorbed part of the incident heat flux becomes smaller and smaller. At the end of the heating period, the absorbed heat flux is seen to be only a few percent of it. The heat flux from the surface during the cooling period is strongly non-linear. During the first 3–4 h the total heat flux from the surface is reduced to half of the starting value, a similar trend to what was observed during the heating period. It is also seen that the heat release by radiation is greater than that by convection. The experimental and theoretical convections are in good agreement, as they should, since the correlation used was that derived by the same instrument and using the same set-up. It should be noted at this point that similar observations were made in the other cases with different incident heat flux densities.

Total heat flux absorbed or released by the surface of the concrete slab,  $q_c$ , is an important

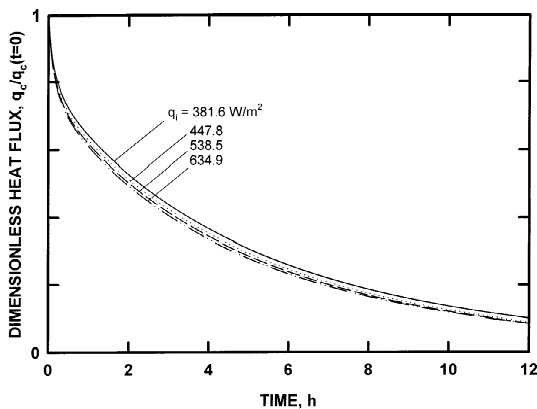


Fig. 8. Theoretical dimensionless heat flux released by surface 1 as a function of time and for various  $q_i$  at the experimental conditions.

parameter, for it shows the transient heat storage or restitution characteristics of the slab. They are calculated at the experimental conditions for all cases and typical results are presented. Non-dimensional total heat flux,  $q_c/q_i$ , during the heating period is plotted as a function of time and for four cases, and the results are shown in Fig. 5. It is seen that the incident heat flux is not a strong parameter affecting the absorbed heat flux by the concrete slab and there seems to be no established trend with it. When all 10 cases were examined, it was seen however that generally  $q_c/q_i$  was a decreasing function of  $q_i$ , which is the expected trend since the surface temperature is an increasing function of it. As a result, the losses are slightly higher; hence the absorbed heat is slightly lower. The reason for the deviation from the expected trend may be attributed to different initial conditions. It is also noted that at the beginning,  $q_c/q_i$  is less than 80%, the reason for which is twofold: the incident heat flux received by the slab surface is only 88% of it, the rest is reflected. Also, the losses by radiation and convection from the surface become considerable right away, since the surface temperature increases immediately as seen in Fig. 3. Following the observation made earlier with Fig. 4, almost half of the incident heat flux is lost after about 3 h from the start. These results show that although energy can be stored more and more by continuing to heat the slab, its storage efficiency will be smaller and smaller. It should also be noted that the thermal loss by radiation makes  $\sim 60\%$  of the total during this period.

The results in Fig. 5 show that in practical situations, the heat storage period could be stopped at a reasonable time. In fact, the stored energy,  $q_{st}$  in  $\text{MJ/m}^2$  and the storage efficiency,  $\eta = q_{st}/q_i$ , are calculated as a function of time from 2 to 12 h for the same conditions of Fig. 4. The results are presented in Fig. 6. The stored energy increases reasonably well at the beginning. During later times, the energy is stored but at smaller rates. In contrast, the efficiency decreases from 74% at  $t=2$  h to 35% at  $t=12$  h, following a power function relationship. The energy storage–restitution may be optimized with respect to storage/restitution time. However this parameter cannot be easily controlled since the heat source may dictate a prescribed operation, such is the case with solar energy applications. Another parameter, the slab thickness for example, may be controlled more easily. This possibility has been studied theoretically for the present experimental conditions and using the same parameters,  $q_{st}$  and

$\eta$  as a function of the slab thickness for  $q_i = 381.6 \text{ W/m}^2$ , at  $t=6 \text{ h}$ . This parametric study is presented in Fig. 7. It is noted that the situation at  $t=6 \text{ h}$  in Fig. 5 represents a beginning of unfavorable conditions, with less energy storage with diminishing thermal efficiency. Yet it is seen that by making the slab thicker, more energy can be stored and at the same time the efficiency can be improved. In fact, by doubling the thickness, the energy storage density is increased by 30% and the thermal efficiency is improved by 6%. Yet other parameters may also be used to maximize the storage–restitution process, such as radiative properties of the receiver surface, like in solar collectors with selective surfaces.

Similarly, the heat flux released by conduction from the slab is non-dimensionalized with respect to the conduction heat flux at  $t=0$  for cooling,  $q_c/q_c(t=0)$  and presented as a function of time in Fig. 8. In this case, the dimensionless heat flux is equal to one at the start and immediately decreases as the cooling progresses. It is seen that, as in the case of heating period, the incident heat flux is not a strong function affecting the dimensionless heat release by the slab. It is noted that there is however a trend with  $q_i$  in this case and an examination of all 10 cases showed that it was also the case when they were included. The reason is of course due to higher surface temperatures obtained with increasing  $q_i$ , which results in higher  $q_c(t=0)$  and in turn,  $q_c/q_c(t=0)$  becomes slightly lower. It is also seen that within about 2 h from the start of cooling period, the total heat flux becomes about one half of the heat flux at the start of the cooling period.

## 6. CONCLUSIONS

Heat transfer by natural convection, conduction and radiation has been studied experimentally on a concrete slab system. Using various hypotheses, a theoretical analysis is also presented. It is seen that the mathematical model developed to predict the thermal performance of the slab system is satisfactory, despite many simplifications made. The natural convection heat transfer correlation derived on the concrete slab was lower by some 18.5% from the correlation generally used in the literature on horizontal surfaces. The reason for the difference is attributed to the uneven heat transfer on a large surface, resulting in lower heat transfer from the center of the plate. The results showed that with the system in this study the incident energy on the concrete slab was not a parameter affecting strongly the absorbed heat by

the slab, the radiation heat losses made about 60% while those by natural convection 40%, and the major energy storage–restitution was taking place during the first 3 to 4 h. The energy storage density and the thermal performance of a system can be optimized by controlling various parameters, including storage–restitution periods, slab thickness and surface radiative properties. The most practical choice could be the slab thickness, although selective surfaces may also be a feasible parameter, especially for solar energy applications.

## NOMENCLATURE

$A$	area, $\text{m}^2$
$c_p$	thermal capacity, $\text{J/kg K}$
$E_b$	black body emissive power, $\text{W/m}^2$
$F_{ij}$	view factor
$H$	concrete slab length, $\text{m}$
$h$	average heat transfer coefficient, $\text{W/m}^2 \text{ K}$
$J$	radiosity, $\text{W/m}^2$
$k$	thermal conductivity, $\text{W/m K}$
$L$	concrete slab thickness, $\text{m}$
$L_c$	$= H \cdot W / (2(H + W))$ , characteristic length, $\text{m}$
$Q$	heat flow rate, $\text{W}$
$q$	heat flux, $\text{W/m}^2$
$Ra$	Rayleigh number, $(g\beta \Delta T L_c^3) / (\nu\alpha)$
$t$	time, $\text{s}$
$T$	temperature, $\text{K}$
$T_\infty$	temperature of surrounding surfaces, $\text{K}$
$T_a$	temperature of surrounding air, $\text{K}$
$W$	concrete slab width, $\text{m}$

### Greek symbols

$\alpha$	thermal diffusivity, $\text{m}^2/\text{s}$
$\beta$	volumetric coefficient of thermal expansion, $1/\text{K}$
$\Delta T$	temperature difference, $(T - T_a)$ , $\text{K}$
$\epsilon$	emissivity
$\nu$	kinematic viscosity, $\text{m}^2/\text{s}$
$\rho$	fluid density, $\text{kg/m}^3$
$\sigma$	Stefan–Boltzmann constant, $5.67 \times 10^{-8} \text{ W/m}^2 \text{ K}^4$

### Subscripts

a	air
b	black body
c	conduction
cv	convection
i	incident
r	radiation
st	stored
1	horizontal surface of the slab
2	heat source surface
3	surrounding surface

*Acknowledgements*—Financial support by Natural Sciences and Engineering Research Council of Canada is acknowledged.



## REFERENCES

- Al-Saad M. A. and Jubran B. A. (1994) Development and testing of concrete solar collectors. *Solar Energy* **16**(1), 27–40.
- Bilgen E. and Michel J. (1979) Integration of solar systems in architectural and urban design. In *Solar Energy Application in Buildings*, Sayigh A. A. (Ed.), Academic Press, New York, Chapter 9.
- Bopshetty S. V. and Nayak J. K. (1992) Performance analysis of a solar concrete collector. *Energy Convers. Manage.* **33**(11), 1007–1016.
- Chaurasia P. B. L. (2000) Solar water heaters based on concrete collectors. *Energy* **25**(8), 703–716.
- Jubran B. A. and Al-Saad M. A. (1994) Computational evaluation of solar heating systems using concrete solar collectors. *Energy Convers. Manage.* **35**(12), 1143–1155.
- Kenny S. P. and Davidson J. H. (1994) Design of a multiple-lamp large-scale solar simulator. *J. Solar Energy Eng.* **116**, 200–205.
- Lloyd J. R. and Moran W. R. (1974) Natural convection adjacent to horizontal surface of various planforms. *J. Heat Transfer* **96**(4), 443–447.
- Nayak J. K., Sukhatme S. P., Limaye R. G. and Bopshetty S. V. (1989) Performance studies on solar concrete collectors. *Solar Energy* **42**(1), 45–56.
- Olive G. (1977) Un nouveau capteur solaire en beton. *Etudes Thermiques et Aerauliques* **8E**(5), 3–14.
- Pretot S., Zeghmati B. and Le Palec G. (2000) Theoretical and experimental study of natural convection on a horizontal plate. *Appl. Thermal Eng.* **20**, 873–891.
- Sedgwick R. H. D. and Patrick M. A. (1981) The use of a ground solar collector for swimming pool heating. In *Proceedings ISES Congress*, Brighton, Vol. 1, pp. 632–636. Pergamon Press.
- Siegel R. and Howell J. R. (1981). *Thermal Radiation Heat Transfer*, McGraw-Hill, New York.
- Sokolov M. and Reshef M. (1992) Performance simulation of solar collectors made of concrete with embedded conduit lattice. *Solar Energy* **48**(6), 403–411.
- Turner R. H. (1986) Concrete slabs as winter solar collectors. In *Proceedings ASME Solar Energy Conference*, pp. 9–13.
- Turner R. H. (1987) Concrete slabs as summer solar collectors. In *Proceedings International Heat Transfer Conference*, pp. 683–689.